JOURNAL OF NATURAL PRODUCTS

Article

pubs.acs.org/jnp

Antibacterial Paramagnetic Quinones from *Actinoallomurus*

Marianna Iorio,*[,†] João Cruz,[‡] Matteo Simone,[†] Alice Bernasconi,[†] Cristina Brunati,[†] Margherita Sosio,[†] Stefano Donadio,[†,‡] and Sonia I. Maffioli[†]

[†]Naicons Srl, Viale Ortles 22/4, 20139 Milano, Italy

[‡]KtedoGen Srl, Viale Ortles 22/4, 20139 Milano, Italy

Supporting Information

ABSTRACT: Four metabolites, designated paramagnetoquinone A, B, C, and D (**1**–**4**), were isolated from three strains belonging to the actinomycete genus *Actinoallomurus*. Compounds **1** and **2** showed potent antibacterial activity with MIC values lower than 0.015 μg/mL against Gram-positive pathogens, including antibiotic-resistant strains. Since compounds **1** and **2** were NMR-silent due to the presence of an oxygen radical, structure elucidation was achieved through a combination of derivatizations, oxidations, and analysis of ^{13}C-labeled compounds. The paramagnetoquinones share the same carbon scaffold as tetracenomycin but carry two quinones and a five-membered lactone fused to the aromatic system. Compounds **2** and **1** are identical except for an unprecedented replacement of a methoxy in **2** by a methylamino group in **1**. Related compounds devoid of methyl group(s) and of antibacterial activity were isolated from a different *Actinoallomurus* strain. The likely *pmq* biosynthetic gene cluster was identified from strain ID145113. While the cluster encodes many of the expected enzymes involved in the formation of aromatic polyketides, it also encodes a dedicated ketoacid dehydrogenase complex and an unusual acyl carrier protein transacylase, suggesting that an unusual starter unit might prime the polyketide synthase.

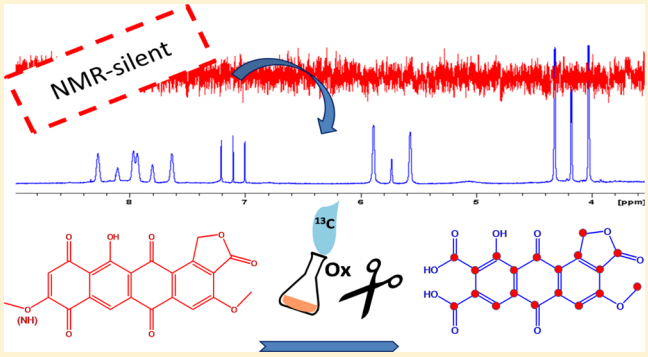

The widespread use of antibacterial agents has led to the selection of resistant pathogens, which represents a serious threat to human well-being and health.[1] This phenomenon is proceeding at a faster pace than our ability to develop safe and effective antibiotics, due to the difficulty of identifying new chemical scaffolds as effective starting points for novel therapeutics. This latter challenge has been exacerbated by a decreased attention to microbial secondary metabolites, which cover a broad chemical space and have been selected through millions of years of evolution.[2] However, the past successes at identifying bioactive molecules from microbial sources make it necessary to devise smart screens in order to identify new metabolites in a time- and resource-effective endeavor.[3] Screening underexplored taxa of microorganisms is a promising approach, since phylogenetic distance from highly explored microbial strains is expected to lead to novel chemistry.

In this respect, we have been focusing on strains belonging to the genus *Actinoallomurus*,[4−7] a member of the *Thermomonosporales* suborder of *Actinobacteria* that was formally described in 2009.[8] The presence of about 1000 such strains in the Naicons collection provides a reasonable number to assess the potential of this genus to yield novel chemistry and, possibly, interesting bioactivities.[3] As part of this effort, we describe herein the paramagnetoquinones **1** and **2** with potent antibacterial activity, together with related metabolites.

RESULTS AND DISCUSSION

Discovery of Paramagnetoquinones. From screening of about 200 *Actinoallomurus* strains, strains ID145113, -145206, and -145754 were identified as producers of related complexes with potent activity against Gram-positive bacteria as well as against a *tolC* mutant of *Escherichia coli*. The strains were isolated from soil samples collected in Corsica (France) and Campania and Emilia Romagna (Italy). On the basis of their 16S rRNA gene sequences, the strains belong to three distinct, previously reported *Actinoallomurus* phylotypes.[4,8]

The active compounds were recovered by precipitation from a concentrated and acidified cleared broth of an ID145113 culture. Washing the resulting pellet with acidified water and drying the residue afforded a black powder that was practically insoluble in water, slightly soluble in organic solvents through the addition of a few drops of HCl or trifluoroacetic acid (yielding a yellow solution), soluble in DMSO, and highly soluble in alkaline aqueous solutions (resulting in a dark purple solution). HPLC analysis showed two major peaks with retention times of 4.1 and 4.2 min (Figure 1, blue trace) in a 4:6 ratio. The UV−vis spectra of **1** and **2** showed absorption maxima at 245, 280, and 455 nm and at 254, 275, and 455 nm, respectively. Both molecules exhibited a characteristic batho-

Received: July 13, 2016
Published: February 20, 2017

DOI: 10.1021/acs.jnatprod.6b00654
J. Nat. Prod. 2017, 80, 819−827

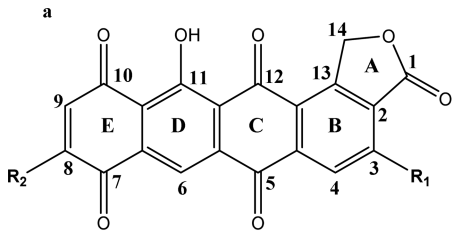

7.

1: R_1=OCH_3, R_2=$NHCH_3$
2: R_1=R_2=OCH_3
3: R_1=R_2=OH
4: R_1=OH, R_2=$NHCH_3$ or R_1=OCH_3, R_2=NH_2

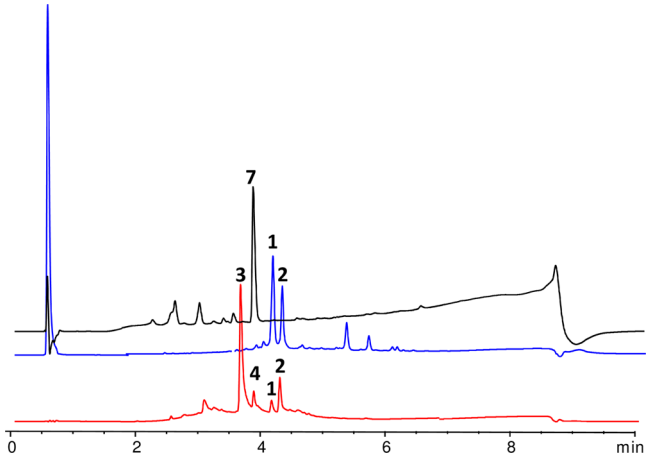

Figure 1. Semipurified extracts from strain ID145113 (blue and black) and ID145206 (red). The blue trace was obtained after precipitation of the cleared broth, while the black trace was from an EtOAc extract of the cleared broth (see Experimental Section).

chromic shift from 455 nm to 550 nm when the pH was raised above 7.0. HR-MS analysis established their chemical formula as $C_{22}H_{14}NO_8$ for **1** and $C_{22}H_{13}O_9$ for **2**.

Structure Elucidation. The **1**/**2** mixture showed the total absence of NMR signals, suggesting the presence of a free radical as previously reported for the so-called *NMR-silent* compounds.[9] In these molecules, the presence of an extended aromatic system containing quinone moieties can lead to severe line-broadening of the NMR signals due to rapid interconversion of the numerous tautomeric forms. An electron paramagnetic resonance (EPR) spectrum of the **1**/**2** mixture gave an intense signal with g = 2.0047 (data not shown), close to the value reported for fredericamycin A,[10] kinobscurinone, and stealthin C[11] and thus consistent with the presence of an oxygen radical. The addition of trifluoroacetic acid (TFA) traces to the NMR sample can sometimes slow down tautomer interconversion and lead to sharp signals, as seen for fredericamycin A.[10] However, this approach was ineffective in our case, so we resorted to the procedure employed for kinobscurinone and stealthins,[11] which required acetylation or methylation of the phenolic oxygens.

Acid-catalyzed acetylation was thus performed on the **1**/**2** mixture, leading to the formation of a mixture of compounds whose m/z ratios were consistent with **1**/**2** carrying multiple acetyls and containing two additional hydrogens, suggesting reduction of a quinone moiety. Specifically, **1** and **2** incorporated up to four and three acetyls, respectively, with the most abundant molecule corresponding to the tri- and diacetyl derivatives of **1** and **2**, respectively. The acetylation mixtures were resolved by preparative TLC, and the purified compounds afforded sharp NMR signals (Supplementary Figure S1). Selected data are reported in Table 1, where Ac-**2** corresponds to diacetyl-reduced-**2** and Ac-**1** corresponds to triacetyl-reduced-**1**. In addition to the signals belonging to the introduced acetyls, whose positions were not investigated, the ^{1}H NMR spectrum of Ac-**2** showed one phenolic proton (14.7 ppm), three aromatic singlets (8.26, 7.85, and 7.67 ppm), one methylene (5.85 ppm), and two methoxy signals (4.11 and 3.98 ppm). Further 2D experiments (Figures S2–S4, Supporting Information) highlighted a NOESY correlation between the aromatic CH at 7.85 ppm and the methoxy group at 4.11. The HMBC correlations between the methyl groups at 3.98 and 4.11 ppm and the carbons at 147.2 and 158.4 ppm, respectively, revealed an aromatic nature for these methoxy groups. Moreover, a carboxyl signal was detected (167.4 ppm) correlating in the HMBC with the methylene at δ_H 5.85. This, in turn, showed a long-range TOCSY correlation with the aromatic CH at δ_H 7.67. HMBC data also showed the presence of two unreduced quinone signals (δ_C 181 and 180.6).

NMR spectra of Ac-**1** (Figures S5 and S6, Supporting Information) showed a similar pattern (see Table 1) except for the presence of a single methoxy (4.23 ppm) and of an additional methyl (3.25 ppm) whose δ_C at 36.1 is consistent with an aromatic methylamino group. Compounds **1** and **2** showed different stability in alkali. In particular, while **1** was stable even at 60 °C for at least 168 h in 0.01 M NaOH, in this solvent **2** readily converted at room temperature into a more hydrophilic compound (t_R 3.9 min and m/z 407 $[M + H]^+$). The 14 amu difference suggested that the *O*-methyl group of **2** was lost under these conditions. An instability of a methoxy in ring E is expected given the negative mesomeric effect brought about by the two quinone oxygens present in the adjacent ring D, which results in a better leaving group in comparison with a methylamino group.[12−14] Altogether, the different stabilities in alkali, the HR-MS data, and the NMR spectra suggested that the difference between **1** and **2** consists in the substitution of a methylamino with a methoxy.

However, the paucity of protons together with the abundance of nonprotonated carbons prevented complete structure elucidation based on the above data. Thus, we resorted to oxidative cleavage of the quinone moiety(ies) performed on native and ^{13}C-enriched **1** and **2**, as detailed below.

In order to break the quinone system and thus eliminate the radical behavior,[15,16] the **1**/**2** mixture was treated with 30% H_2O_2 in water (Scheme 1). Within 1 h at room temperature, the starting dark purple solution turned yellow with the formation of a single, more hydrophilic molecule (compound **5**) with an m/z of 399 $[M + H]^+$ and UV absorptions at 230, 280, and 420 nm (Figure S7, Supporting Information). This result indicated that the oxidation had removed the portion responsible for the difference between **1** and **2**. As expected,

DOI: 10.1021/acs.jnatprod.6b00654
J. Nat. Prod. 2017, 80, 819−827

Table 1. Selected NMR Spectroscopic Data (400 MHz) for Compounds Ac-2, Ac-1, and Ac-3 ($CDCl_3$) and 7 (CD_3OD)

	Ac-2[a]		Ac-1[a]		Ac-3[a]		7[b]	
position	δ_C, type	δ_H, mult	δ_C, type	δ_H, mult	δ_C, type	δ_H, mult	δ_C, type	δ_H, mult (J in Hz)
1	167.4, C		166.4, C		166.1, C			
2	119.4, C		nd[c]		nd		43, CH_2	2.16, m
3	158.4, C		162.9, C		nd		62.5, CH	4.16, m
4	122.4, CH	7.67, s	124,2, CH	7.49, s	122.1, CH	8.14, s	40, CH_2	2.80, dd (16.7−7.8) 3.13, dd (16.7−4.5)
4a	140, C		nd		nd		146, C	
5	181, C		nd		nd		120, CH	7.53, s
5a	nd		nd		nd		nd	
6	120.1, CH	8.26, s	nd	8.41, s	116.1, CH	8.35, s	180.6, C	
6a	nd		nd		nd		nd	
7	180.6, C		nd		nd		107.6, CH	7.30, d (2.5)
8	147.2, C		nd		nd		166.6, C	
9	108.7, CH	7.85, s	108.7, CH	7.91, s	119.9, CH	7.34, s	106, C	6.77, d (2.5)
10	nd		nd		nd		166.4, C	
10a	110.9, C		nd		nd		110, C	
11	nd		nd		nd		181.6, C	
11a	120.8, C		nd		nd		114, C	
12	nd		nd		nd		nd	
12a	119.4, C		nd		nd		133, C	
13	nd		nd		nd		75, C	
14	70.9, CH_2	5.85, s	70.6, CH_2	5.77, s	71.1, CH_2	5.81, s	67, CH_2	3.7, d (10.6) 4.46, d (10.6)
OCH_3-3	56.5, CH_3	4.11, s	57.2, CH_3	4.23, s				
OCH_3-8	61.3, CH_3	3.98, s					56, CH_3	3.95, s
$NHCH_3$-8			36.1, CH_3	3.25, s				
OH-11		14.75, s		15.01, s		14.86, s		

[a]These molecules also show signals between 20.5 and 21 (δ_C) and between 2.3 and 2.6 (δ_H) corresponding to the chemically introduced acetyls. [b]Phenolic signals are not detectable under these conditions. [c]nd: not detected.

Scheme 1. Oxidative Cleavage of Paramagnetoquinones

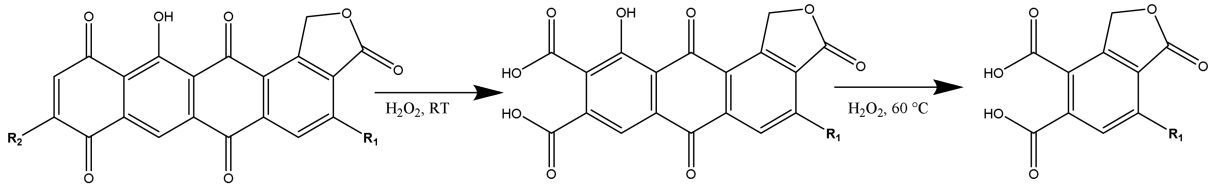

1: R_1=OCH_3, R_2=$NHCH_3$
2: R_1=R_2=OCH_3
3: R_1=R_2=OH

5: R_1=OCH_3
8: R_1=OH

6: R_1=OCH_3
9: R_1=OH

purified **5** was no longer paramagnetic and clear ^{1}H NMR signals were observed (Table 2; Figure S8, Supporting Information): one broad phenolic signal (12.48 ppm), two aromatic protons at 8.14 and 7.81 ppm, one methylene signal at 5.73 ppm, and one methoxy group at 4.18 ppm. Overall, the MS data, the absence of one aromatic proton and of one methoxy group in **2** (or one methylamino in **1**), are in agreement with a terminal quinone moiety oxidatively cleaved and replaced by two carboxylic acids as reported in the literature.[15,16]

Sufficient incorporation into paramagnetoquinones of ^{13}C-labeled precursor(s) took some media design efforts, since attempts failed in a minimal medium suitable for growth of and paramagnetoquinone production by strain ID145113 (see Experimental Section). We thus resorted to remove and/or replace individual components from the complex AF-A production medium in order to render it closer to a chemically defined medium. Replacing soy flour with glutamine and reducing the yeast extract concentration to 0.5% (resulting in AF-N medium) led to satisfactory growth and paramagnetoquinone production of about 400 μg/mL after 8 days of cultivation.

Strain ID145113 was thus cultivated in 200 mL of AF-N medium containing ^{13}C-[U]-glucose. LC-MS analysis indicated that paramagnetoquinones were about 80% enriched in ^{13}C. Purification as described above led to 45 mg of the **1**/**2** mixture, which was then treated with H_2O_2 to obtain ^{13}C-labeled **5**.

NMR analysis (HSQC, HMBC, together with ^{13}C, ADEQUATE, and INADEQUATE; Figures S9−S11, Supporting Information) of ^{13}C-**5** allowed detection of all non-protonated carbons. Three carbonyl signals at 166.7, 166.5, and 165.5 confirmed the presence of the two oxidation-generated carboxylic acids, together with the carbonyl moiety that showed HMBC correlation with the CH_2 group, as seen with the acetylated derivatives. Two signals, at 187.4 and 181 ppm, evidenced the presence of an intact quinone not affected by

DOI: 10.1021/acs.jnatprod.6b00654
J. Nat. Prod. 2017, 80, 819−827

Table 2. NMR Spectroscopic Data (DMSO-d_6/TFA, 9:1) for Compound 5

position	δ_C, type	δ_H	HMBC	INADEQUATE	ADEQUATE
1	166.7, C			2	
2	118.2, C			1, 3	
3	163, C			2, 4	
4	110, CH	7.81, s	2, 5, 11a, 12a	3	3, 4a
4a	140.1, C			5	
5	181, C			4a, 5a	
5a	133.7, C			5, 6	
6	119.5, CH	8.14, s	5, 7, 10a, 12a	5a, 6a	5a, 6a
6a	134.9, C			6, 7	
7	165.5, C			6a	
10	166.5, C			10a	
10a	132.1, C			10, 11	
11	158.1, C			10a	
11a	120.9, C			12	
12	187.4, C			11a	
12a	117.9, C			13	
13	152.9, C			12a, 14	
14	70.8, CH_2	5.73, s	1, 2, 4a, 11a, 12a, 13	13	13
15	57.7, CH_3	4.18, s	3		
OH-11		12.48, brd			

oxidation and presumably internal to the remaining aromatic system. The connectivity of the carbon atoms of the central core was assigned by INADEQUATE and 1,1-ADEQUATE experiments (Figure 2). Substitutions at positions 3 and 11

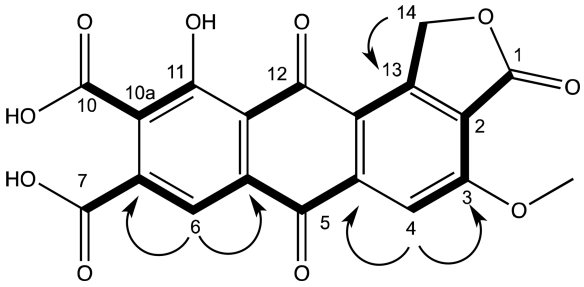

Figure 2. Chemical structure of compound 5 with INADEQUATE (bold) and 1,1-ADEQUATE (arrows) correlations.

were thus clearly assigned to the methoxy and hydroxy groups, respectively, with the lactone ring confirmed to be fused to the B ring at positions 2−13.

Subjecting 5 to stronger oxidation conditions (30% H_2O_2 at 60 °C for 14 h, Scheme 1) led to the formation of a more hydrophilic compound (t_R 2.1 min; m/z of 253 $[M + H]^+$; UV maxima at 220, 260, and 304 nm; Figure S7, Supporting Information), consistent with cleavage of the internal quinone moiety of 1 and 2 and formation of the compound shown in Scheme 1.

Antibacterial Activities. The antibacterial activities of the mixture 1/2 are reported in Table 3. The mixture showed MIC values in the range 0.03−0.25 μg/mL against *Enterococcus* and *Staphylococcus* spp., with good activity also against all antibiotic-resistant strains tested. Against *Streptococcus* spp. the MICs were lower than 0.015 μg/mL. Activity was also seen against one fast-growing mycobacterium, the *E. coli* Δ*tolC* strain, and one *Moraxella catarrhalis* strain (MICs of 0.5, 1, and 0.03 μg/mL, respectively). The mixture 1/2 was active against some anaerobic bacteria (*Lactobacillus delbrueckii*, *Bacteroides fragilis*, and *Propionibacterium acnes*; MICs of 0.5−1 μg/mL) but not against *Clostridium difficile* (a single strain tested). No activity (MIC > 16 μg/mL) of 1 and 2 was observed against the other tested Gram-negative strains (Table 3) or against *Candida* spp. Compound 5 was devoid of detectable activity against the strains from Table 3.

Related Metabolites from Other *Actinoallomurus* Strains. Compounds indistinguishable from 1 and 2 were also found in the fermentation broth of strain ID145754 (data not shown), as well as minor congeners in the fermentation broth of strain ID145206, which produced 3, with m/z 393 $[M + H]^+$, as the main compound. As mentioned above, the three *Actinoallomurus* strains belong to three distinct phylotypes. The structure of 3, which was also NMR silent, was elucidated following the same purification and derivatization procedure applied to 1 and 2. In this case, acetylation resulted in the formation of a tetra-acetyl-reduced derivative as the main product, with up to five added acetyls observed in the reaction mixture. ^1H and 2D NMR experiments of the purified major acetylated compound (Figures S12 and S13, Supporting Information) evidenced the presence of one phenol (14.86 ppm), three aromatic protons (8.35, 8.14, and 7.34 ppm), and a CH_2 (5.81 ppm), with the absence of methyl groups, apart from the acetyl-associated methyls. Acetylated 3 showed a long-range TOCSY correlation between the CH_2 and one of the aromatic protons (δ_H 8.14, δ_C 122.1). Selected data are listed in Table 1. H_2O_2 oxidation at room temperature or at 60 °C converted 3 into more hydrophilic products with m/z 385 $[M + H]^+$ or m/z 239 $[M + H]^+$, respectively, consistent with compounds 8 and 9 in Scheme 1. Thus, the main metabolite from strain ID145206 corresponds to 2 lacking the two *O*-methyls in the B and E rings. As expected, 3 was stable in alkaline conditions. Surprisingly, 3 was virtually devoid of activity against all tested strains, except for streptococci, for which the observed MICs were 3 orders of magnitude higher than those of the 1/2 mixture (see Table 3). Thus, the methyl groups present in 1/2 are important for antibacterial activity. It should be noted that strain ID145206 also produced a lesser amount of the related compound 4, with m/z 406 $[M + H]^+$, a similar UV−vis spectrum to 1, and which was stable in alkaline

DOI: 10.1021/acs.jnatprod.6b00654
J. Nat. Prod. 2017, 80, 819−827

Table 3. Antimicrobial Activities of Paramagnetoquinones, Vancomycin (Van), and Gentamicin (Gen) against Gram-Positive and Gram-Negative Bacteria Expressed as MIC Values

		MIC (μg/mL)			
strain	code	**1**/**2**	**3**	Van	Gen
Staphylococcus aureus Met-S	ATCC6538P	0.125	>16	0.5	
Staphylococcus aureus Met-R	L1400	0.125	>16	1	
Staphylococcus aureus GISA	L3797	0.25	>16	8	
Staphylococcus aureus GISA	L3798	0.125	>16	8	
Staphylococcus hemolyticus Met-S	L1729	0.06	>16	2	
Staphylococcus hemolyticus Met-R	L1730	0.25	>16	128	
Streptococcus pyogenes	L49	≤0.015	16	0.5	
Streptococcus pyogenes	ATCC BAA 1407	≤0.015	8	0.5	
Streptococcus pyogenes	ATCC BAA 1402	≤0.015	8	0.5	
Streptococcus pyogenes	ATCC49619	≤0.015	8	0.5	
Enterococcus faecium VanS	L568	0.03	>16	2	
Enterococcus faecium VanA	L569	0.06	>16	>128	
Mycobacterium smegmatis	mc^2 155	0.5	>16	>128	16
Escherichia coli Δ*tolC*	L4242	1	>16	>128	0.25
Escherichia coli hyperpermeable	G1640	0.5	>16	>128	0.25
Escherichia coli	ATCC25922	>16	>16	>128	0.25
Moraxella catarrhalis	L3292	0.03	>16	32	0.25
Haemophilus influenzae	L3296	>16	>16	>128	128
Pseudomonas aeruginosa	ATCC27853	>16	>16	2	0.5
Acinetobacter baumannii	ATCC13637	>16	>16	128	0.125
Stenotrophomonas maltophilia	L3030	>16	>16	128	64
Lactobacillus delbrueckii	ATCC4797	1	>16	>128	
Bacteroides fragilis	ATCC25285	1	>16	16	
Propionibacterium acnes	ATCC25476	0.5	>16	0.25	
Clostridium difficile	L4013	>16	>64	0.5	

conditions. These data are consistent with **4** being identical to **1**, containing just one of the methyl groups. Thus, strain ID145206 is producing a complex sharing the same scaffold as **1** and **2** but, under the investigated experimental conditions, is inefficient at performing methylations.

Overall, paramagnetoquinones share the same polyketide scaffold as tetracenomycins but with key differences, including two quinones, in rings C and E, instead of the single quinone in ring D, a five-membered lactone ring fused to ring B, and a paucity of postpolyketide oxidations. A quinone in a methoxy-carrying terminal ring is present in several metabolites with different polyketide scaffolds (e.g., fredericamycin, polyketomycin, dutomycin, cervymycin, and bikaverin). Five-membered lactone rings can be found, in linear or angular positions, in some aromatic polyketides (e.g., austrocorticins, araliolactones, and allocyclinone). However, this feature was never reported for a tetracenomycin analogue, which only presented a methyl group at the 14-corresponding position, with some congeners carrying a carboxyl group at the 1- corresponding position. The unique feature of paramagnetoquinones is the existence of two congeners, produced in equivalent amounts, which differ for either an *N*-methyl or O-methyl group in ring E. The presence of an *N*-methyl in an equivalent position has been reported for a naphthoquinone from *Streptomyces*, but no *O*-congeners were detected in that case.[17] Despite the similarities to the tetracenomycin family, paramagnetoquinones show different antimicrobial behavior with MIC values 3 orders of magnitude lower than tetracenomycins against both staphylococci and enterococci.[18]

A Likely Biosynthetic Intermediate. Having established that paramagnetoquinones share the same carbon scaffold with the tetracenomycin family, we further looked for related metabolites in cultures of strain ID145113. By extracting the cleared broth with ethyl acetate, then back-extracting the organic phase with 0.05 M NaOH, about 2 mg of the purple compound **7** was isolated. LC-MS analysis showed a peak at t_R 3.8 min with an m/z of 387 $[M + H]^+$ (Figure 1, black chromatogram). After dissolution in CD_3OD, NMR analysis showed sharp and clear signals, indicating that this metabolite was radical-free. Selected ^1H and ^{13}C NMR data are reported in Table 1. A clear aliphatic spin system evidenced the presence of a nonaromatic hydroxylated ring, carrying a hydroxymethylene. Further signals included two aromatic protons (at 7.3 and 6.77 ppm) in meta position (J = 2 Hz) and one aromatic proton (7.53 ppm) as an isolated singlet. A quinone moiety was revealed by the presence of an HMBC correlation between the proton at 7.53 and a carbon at 180.6 ppm. A methoxy group at 3.95 ppm correlated in the HMBC with an aromatic carbon at 166.6 ppm and in the NOESY with the aromatic proton at 6.77 ppm. A NOESY correlation was also visible between the signals at 7.53 and 2.80 ppm, the latter corresponding to one of the protons of C4, the methylene of the aliphatic ring directly connected to the aromatic rings. The two proton in meta position correlated with a carbon at 110 ppm, consistent with C10a. Moreover, one of the protons at C14 (at 3.72 ppm) correlated in the HMBC with a carbon at 133 ppm, which was the same carbon seen by the aromatic proton at 7.53 ppm, demonstrating that the aliphatic ring B was linearly fused with the aromatic ring C. Overall, the combined LC-MS and NMR data are consistent with the structure of compound **7** as shown: **7** shares the same polyketide backbone as **1** and **2**, but the terminal carboxyl group has been lost. Interestingly, **7** has not yet undergone aromatization of ring B and, in contrast with **1** and **2**, monooxygenation has occurred in the central ring.

DOI: 10.1021/acs.jnatprod.6b00654
J. Nat. Prod. 2017, 80, 819−827

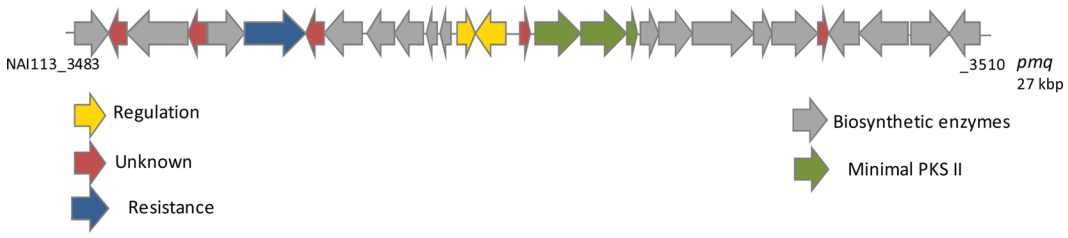

Figure 3. *pmq* gene cluster. *pmq* genes are grouped by category as indicated and as listed in Table 4.

Table 4. Deduced Function of Each CDS in the *pmq* Biosynthetic Gene Cluster

pmq CDS[a]	length (aa)	predicted function[b]	cluster (protein)	accession no.	e value	identity (%)
NAI113_3483	390	oxidoreductase	validamycin (ValF)	ABA41510.1	3e-49	32
NAI113_3484	175	unknown	no hits			
NAI113_3485	534	bilirubin oxidase	xantholipin (XanP)	ADE22283.1	3e-166	50
NAI113_3486	151	unknown	lysolipin (LlpQ)	CAM34365.1	7e-36	50
NAI113_3487	330	malonylCoA ACP transacylase	bacillaene (BaeD)	CAG23951.1	2e-60	35
NAI113_3488	621	drug resistance transporter	FD-594 (PnxT)	BAJ52670.1	4e-116	39
NAI113_3489	127	unknown	dynemicin (ORF35)	ACB47077.1	5e-13	35
NAI113_3490	431	E2 dihyrolipoyl acyltrasferase	tetronasin (Tsn2)	ACR50769.1	2e-140	38
NAI113_3491	344	transketolase	tetronasin (Tsn3)	ACR50770.1	8e-124	55
NAI113_3492	327	dehydrogenase E1 component	tetronasin (Tsn4)	ACR50771.1	2e-140	67
NAI113_3493	130	monooxygenase	lysolipin (LlpOIII)	CAM34339.1	8e-31	42
NAI113_3494	107	polyketide synthesis cyclase	tetracenomycin (TcmI)	AAA67513.1	1e-33	46
NAI113_3495	184	PadR regulatory protein	chromomycin (CmmRII)	CAE17541.1	4e-29	36
NAI113_3496	287	SARP regulatory protein	griseorhodin (GrhR2)	AAM33680.1	9e-81	47
NAI113_3497	123	unknown	lactonamycin Z (Lcz30)	ABX71147.1	4e-48	52
NAI113_3498	421	KSα	arimetamycin (Arm7)	AHA81977.1	0e+00	69
NAI113_3499	432	KSβ	oviedomycin (OvmK)	CAG14966.1	0e+00	63
NAI113_3500	84	ACP	actinorhodin (ActI-3)	AAK06786.1	5e-27	53
NAI113_3501	155	cyclase/dehydratase	rubromycin (RubF)	AAG03070.2	2e-81	73
NAI113_3502	349	*O*-methyltransferase	elloramycin (ElmNII)	CAP12604.1	6e-110	51
NAI113_3503	576	ACC, carboxyl transferase	R1128 (ZhuF)	AAG30193.1	0e+00	61
NAI113_3504	167	BCCP	polyketomycin (PokAC3)	ACN64838.1	2e-36	45
NAI113_3505	452	ACC, biotin carboxylase	dactylocycline (DacP1)	AFU65905.1	0e+00	66
NAI113_3506	53	unknown	no hits			
NAI113_3507	357	*O*-methyltransferase	polyketomycin (pokMT2)	ACN64843.1	8e-77	41
NAI113_3508	562	hydroxylase	tetracenomycin (TcmG)	AAA67511.1	1e-163	47
NAI113_3509	331	*O*-methyltransferase	GE2270 (PbtM4)	AGY49596.1	2e-102	53
NAI113_3510	299	NmrA family protein	pristinamycin (c104_12)	CBW45633.1	2e-59	44
NAI113_3511	n.a.	tRNA Pro GGG	n.a.			

[a]Bold type indicates *pmq* CDSs that show the highest BLAST score with sequence from a PKS II cluster listed in the MIBIG database. [b]Abbreviations: ACC, acetylCoA carboxylase; ACP, acyl carrier protein; BCCP, biotin carboxylate carrier protein; KSα, type II polyketide synthase β-ketoacyl synthase, alpha subunit; KSβ, type II polyketide synthase β-ketoacyl synthase, beta subunit.

Nonetheless, **7** already carries the hydroxymethylene group, which results in the ring A in mature **1** and **2**. We were unable to detect a compound corresponding to the amino version of **7** in fermentation broths, suggesting that **2**, or a precursor, can be converted into the amino form **1** only after a quinone moiety has been installed in ring E.

The Likely *pmq* Gene Cluster. We were interested in exploring whether the gene cluster responsible for paramagnetoquinone formation would provide insights into its unusual structural features, in particular the presence of a nitrogen or oxygen atom at position 8. From a draft genome sequence of strain ID 145113,[19] we readily identified a single gene cluster (designated *pmq*) encoding the expected PKS II system flanked by a tRNA-Pro gene on one end. The *pmq* gene cluster encompasses a DNA region of about 27 kbp and consists of at least 10 transcription units (Figure 3). The predicted roles for the identified coding DNA sequences (CDSs) are described in Table 4. When probed against the MIBiG database, about two-thirds of the CDSs in the cluster had a higher pairwise similarity to sequences from other type II PKS clusters. These included the expected minimal PKS (NAI113_3498-_3500) for the synthesis of the decaketide precursor, two cyclases (NAI113_3493 and _3501), and one TcmG-like monooxygenase (NAI113_3508), likely responsible for introducing the oxygen at C-7.[20] Surprisingly, while **1** and **2** each carries just two methyl groups, the *pmq* cluster encodes three methyltransferases: NAI113_3502, showing 51% identity to the elloramycin/tetracenomycin TcmN-type sequences and likely to be responsible for *O*-methylation at position 8,[21] NAI113_3507, showing 45% identity to the polyketomycin methyltransferase PokMT2, predicted to be a C-methyltransferase,[22] and NAI113_3509, closely related to PbtM4 (53% identity), involved in thiazole *O*-methylation in the thiopeptide GE2270[23] (see Table 4).

DOI: 10.1021/acs.jnatprod.6b00654
J. Nat. Prod. 2017, 80, 819−827

While the *pmq* cluster does not encode any candidate for introducing the nitrogen atom at position 8, it does encode unusual features, namely, the three components of a biotin-dependent carboxylase (NAI113_3503-_3505) for generating the malonyl-CoA extender units, a PKS-related acyltransferase (NAI113_3487), presumably involved in charging the ACP with a starter/extender unit, and an apparently functional ketoacid dehydrogenase complex (NAI113_3490-_3492), presumably responsible for generating an acyl-CoA precursor. Surprisingly, the acyltransferase NAI113_3487 is more related to the equivalent domains from type I PKSs from *Proteobacteria* than to actinomycete-derived PKSs (Table 4).

Thus, the *pmq* cluster appears to encode enzymes involved in the formation of two sets of CoA derivatives, one by carboxylation of acetylCoA and the other by decarboxylation of a ketoacid. The presence of an acyl-CoA-generating system and of an acyltransferase within the *pmq* cluster are consistent with the possibility that a special polyketide unit is produced by the ketoacid dehydrogenase complex and charged onto the ACP by the acyltransferase NAI13_3487. Since **1** and **2** contain a hydroxymethyl group at a place equivalent to the polyketide starter unit in tetracenomycin and since the hydroxymethyl is already present in the metabolite **7**, it is possible that paramagnetoquinone biosynthesis utilizes a hydroxyacetyl-CoA as starter unit.

EXPERIMENTAL SECTION

General Experimental Procedures. LC-MS analysis were performed with an Agilent 1100 Series liquid chromatograph equipped with an Ascentis Express Supelco RP18, 2.7 μm, 50 × 4.6 mm, column eluted at 1 mL/min at 40 °C. Elution was with a 10 min multistep program that consisted of 5%, 95%, 100%, and 5% phase B at 0, 6, 7, and 7.2 min, respectively (phases A and B were 0.05% TFA [v/v] in water and in acetonitrile, respectively) with detection at 220 nm. The effluent from the column was split 1:1 into a photodiode array detector and into the ESI interface of a Bruker Esquire 3000 Plus ion trap mass spectrometer (Bruker). Mass spectrometry analysis was performed using the following sample inlet conditions: sheath gas (N_2) 50 psi, dry gas 10 L/min, capillary heater 365 °C; sample inlet voltage settings: positive polarity, capillary voltage −4000 V, end plate offset −500 V; scan conditions: maximum ion time 200 ms, ion time 5 ms, full microscan 3; segment: duration 10 min, scan events positive (100−2400 *m*/*z*). HR-MS analyses were performed on an Exactive benchtop mass spectrometer (Thermo Fisher Scientific Spa, Milano, Italy), equipped with a nanospray ionization/electrospray ionization ion source by direct infusion of compounds dissolved in DMSO/H_2O, 1:9. The EPR spectrum was measured using a Bruker Elexys spectrometer, equipped with an ER4102ST standard rectangular cavity. The loose-packed sample was loaded in a cylindric quartz tube (Covaler, i.d. 3 mm, o.d. 4 mm). The magnetic field intensity was monitored by a teslameter. The EPR spectrum was collected at a working frequency of 9.4047 GHz (as measured by an HP5340A frequency counter). ^{1}H and ^{13}C 1D and 2D NMR spectra (COSY, TOCSY, NOESY, HSQC, HMBC) were measured in $CDCl_3$ or DMSO-d_6 with or without TFA addition at 25 °C using a Bruker AMX 400 MHz spectrometer. Adequate and inadequate experiments were measured on an Agilent (Varian) VNMRS 500 MHz spectrometer.

Producer Strains and Cultivation Conditions. *Actinoallomurus* ID145113, ID145206, and ID145754 were maintained on S1 5.5 plates.[4] The strains were grown in shake-flasks containing AF-A medium (dextrose 10 g/L, soybean meal 4 g/L, yeast extract 1 g/L, NaCl 0.5 g/L, MES 1.5 g/L, adjusted to pH 5.6 before sterilization) for 240 h at 30 °C in a rotatory shaker at 200 rpm. For ^{13}C-labeling experiments, an exponentially growing culture of strain ID145113 in AF-A medium was inoculated (10%) in AF-N medium (^{13}C-glucose 5 g/L, glutamine 1 g/L, yeast extract 0.5 g/L, NaCl 0.5 g/L, MES 1 g/L, adjusted to pH 5.6 before sterilization). Amplification and analysis of 16S rRNA gene sequences were performed as previously described[4,24] (deposited in GenBank with accession numbers KX533972, KX533973, and KX533974 respectively for strains ID145113, -145206, and -145754).

Metabolite Purification. A 2 L culture of strain ID145113 was harvested and centrifuged at 3000 rpm for 10 min to separate the mycelium from the clear broth. The latter (about 1.8 L) was concentrated under vacuum to about 1 L and brought to pH 3.2 with 7.2 mL of 6 N HCl. The suspension was kept overnight at 4 °C, and the resulting pellet was collected by centrifugation at 4000 rpm for 10 min, washed twice with 0.1 N HCl (5 mL), and dried in a vacuum oven at 40 °C for 48 h, yielding 595 mg of a black powder containing **1** and **2**. HR-MS analysis established their chemical formula as $C_{22}H_{14}NO_8$ for **1** (420.0714 found, 420.0719 calcd) and $C_{22}H_{13}O_9$ for **2** (421.0557 found, 421.0559 calcd). The same downstream process was applied to a 200 mL culture of strain ID145113 grown in ^{13}C-labeled medium, providing 42 mg of ^{13}C-labeled **1**/**2** mixture. For **3**, 56 mg was similarly obtained from a 200 mL culture of strain ID145206. Compound **7** was purified from a 1 L culture of strain ID145113. After centrifugation as above, the supernatant was extracted twice with 500 mL of ethyl acetate; then the organic phase was reduced to 200 mL and extracted twice with 100 mL of 0.05 N NaOH. The aqueous phase was evaporated under reduced pressure, and about 2 mg of **7** was isolated as a purple powder.

Acetylation, Oxidation, and Stability. To a dark brown, colloidal solution of **1**/**2** (50 mg) in acetic anhydride (3 mL) was added pure H_2SO_4 (10 μL). The mixture was kept at room temperature with stirring for 10 h. The color slowly turned yellow. The reaction was quenched with the addition of 4 mL of H_2O and extracted twice with 6 mL of ethyl acetate. The organic phase was dried. TLC on silica gel (Fluka Analytical) with CH_2Cl_2/CH_3OH (98:2 v/v) showed at least four spots. These were separated by preparative TLC on silica gel to afford the most abundant corresponding to the triacetyl derivative of **1** (3.9 mg) and the diacetyl derivative of **2** (4.8 mg). NMR analysis of both products was carried out in $CDCl_3$. The same reaction was conducted on 15 mg of **3**, obtaining 2.3 mg of tetraacetyl derivative.

The **1**/**2** mixture (20 mg) was dissolved in 4 mL of 30% H_2O_2 and 2 mL of acetonitrile and kept under magnetic stirring for 24 h. After complete conversion of **1**/**2** into **5** (t_R 3.6 min with *m*/*z* of 399 $[M + H]^+$ and UV absorptions at 230, 280, and 420 nm), the reaction was quenched with the addition of 400 μL of 1 M sodium metabisulfite and concentrated under vacuum. **5** was purified using a CombiFlash RF Teledyne ISCO medium-pressure chromatography system on a 30 g Biotage SNAP Cartridge KP-C_{18}-HS. The column was previously conditioned at 10% phase B, brought to 25% phase B in 2 min, then eluted at 30 mL/min for 10 min up to 45% phase B. After elution, the column was washed with 80% phase B (phase A was water with 0.1% TFA, and phase B was acetonitrile). Fractions containing **5** were pooled and dried under reduced pressure, obtaining 6 mg of purified compound. The same reaction was conducted on 42 mg of a 70% ^{13}C-labeled **1**/**2** mixture, obtaining 20 mg of ^{13}C-**5**. Unlabeled **5** was also subjected to reaction with 30% H_2O_2 at 60 °C for 14 h, obtaining **6** (t_R 2.4 min, *m*/*z* of 253 $[M + H]^+$, UV absorption peaks at 220, 260, and 304 nm). Compound **3** (2 mg) was reacted with 30% H_2O_2 (room temperature, 1 h), giving compound **8** (t_R 3.0 min, *m*/*z* of 385 $[M + H]^+$), which was then converted into **9** (t_R 2.3 min, *m*/*z* of 239 $[M + H]^+$) after treating with H_2O_2 at 60 °C for 14 h. For NMR characterization, 5 mg of **5** was dissolved in 450 μL of DMSO-d_6/50 μL of TFA.

The **1**/**2** mixture (1 mg) was dissolved in 1 mL of 0.01 M NaOH, yielding a dark purple solution and monitored by LC-MS over time. At room temperature, about 50% **2** converted in 24 h into a more hydrophilic derivative (t_R 3.9 min, *m*/*z* 407 $[M + H]^+$). At 60 °C, **2** completely converted within 20 min into a 407 *m*/*z* compound. Under both conditions, **1** was stable, as was the **3**/**4** mixture (tested only at 60 °C).

*Paramagnetoquinone A (**1**):* purple powder; UV−vis (0.1% TFA/acetonitrile, 3:7) λ_{max} (log ε) 245 (5.25), 285 (5.30), 455 (4.79) nm; NMR silent; EPR data: *g* = 2.0047; ESI(+)MS *m*/*z* 420.1 $[M + H]^+$;

DOI: 10.1021/acs.jnatprod.6b00654
J. Nat. Prod. 2017, 80, 819−827

HRESI(+)MS m/z 420.0714 $[M + H]^+$ (calcd for $C_{22}H_{14}NO_8$, 420.0719).

Paramagnetoquinone B (2): purple powder; UV−vis (0.1% TFA:/acetonitrile, 3:7) λ_{max} (log ε) 254 (5.27), 274 (5.33), 455 (4.73) nm; NMR silent; EPR data: g = 2.0047; ESI(+)MS m/z 421.2 $[M + H]^+$; HRESI(+)MS m/z 421.0557 $[M + H]^+$ (calcd for $C_{22}H_{13}O_9$, 421.0559).

Paramagnetoquinone C (3): purple powder; UV−vis (0.1% TFA/acetonitrile, 3:7) λ_{max} (log ε) 240 (5.03), 273 (5.20), 455 (4.59) nm; NMR silent; ESI(+)MS m/z 393.2 $[M + H]^+$; HRESI(+)MS m/z 393.0829 $[M + H]^+$ (calcd for $C_{20}H_9O_9$, 393.0241).

Triacetyl paramagnetoquinone A: yellow powder; ^1H and ^{13}C NMR data, Table 1; ESI(+)MS m/z 548.1 $[M + H]^+$.

Diacetyl paramagnetoquinone B: yellow powder; ^1H and ^{13}C NMR data, Table 1; ESI(+)MS m/z 507.2 $[M + H]^+$.

Oxidized derivative (5): orange powder; UV−vis (0.1% TFA/acetonitrile, 3:7) λ_{max} (log ε) 230 (5.27), 280 (5.07), 420 (4.49) nm; ^1H and ^{13}C NMR data, Table 2; ESI(+)MS m/z 399 $[M + H]^+$.

Biosynthesis intermediate of paramagnetoquinones (7): purple powder; ^1H and ^{13}C NMR data, Table 1; ESI(+)MS m/z 387 $[M + H]^+$.

Bioinformatic Analysis. Identification of biosynthetic gene clusters was performed using the Antismash v3.0.1 tool at the default conditions.[25] BLAST analysis of individual CDSs was performed against the MIBiG database of known gene clusters.[26] The sequence of the *pmq* cluster has been deposited with accession number KX533975.

Antimicrobial Assays. Minimal inhibitory concetrations (MICs) were determined according to CLSI guidelines[27] by broth microdilution in sterile 96-well microtiter plates, using Müller Hinton broth containing 20 mg/L $CaCl_2$ and 10 mg/L $MgCl_2$ for all aerobic bacteria except for *Streptococcus* spp., *Mycobacterium smegmatis*, and *Haemophilus influenzae*, which were grown in Todd Hewitt broth, in Middlebrook 7H9 broth (with 10% OADC supplement, BD, Becton Dickinson, USA), and Brain Hearth Infusion (with 0.5% yeast extract), respectively. Anaerobes were grown in *Brucella* broth supplemented with 5 μg/mL hemin and 1 μg/mL vitamin K1, with Oxyrase (Oxyrase Inc., Mansfield, OH, USA) added (1:25 v/v) when growing *Clostridium* spp. All media were from Difco Laboratories. Strains were inoculated at 5×10^5 cfu/mL. Aerobic bacteria were incubated at 37 °C for 20−24 h, with the exception of *Mycobacterium smegmatis* strain, which required a 72 h incubation. Anaerobes were incubated at 37 °C for 48 h in a plastic GasPak EZ incubation container system with anaerobic conditions (80% N_2, 10% CO_2, and 10% H_2) obtained with a GasPaK EZ Gas generating sachet (BD, Becton Dickinson, USA). All strains (with the exception of the ATCC strains and mc^2155) were clinical isolates from the NAICONS strain collection.

■ ASSOCIATED CONTENT

Supporting Information

The Supporting Information is available free of charge on the ACS Publications website at DOI: 10.1021/acs.jnatprod.6b00654.

^1H NMR spectra of Ac-**1**, Ac-**2**, Ac-**3**, and ^{13}C-labeled **5**; NOESY spectrum of compound Ac-**2**; HSQC spectra of Ac-**1**, Ac-**2**, and Ac-**3**; HMBC spectrum of Ac-**2**; ^{13}C NMR spectrum, ADEQUATE, and INADEQUATE of ^{13}C-labeled **5**; HPLC chromatograms and UV spectra of compounds **5** and **6** (PDF)

■ AUTHOR INFORMATION

Corresponding Author

*E-mail: miorio@naicons.com.

ORCID

Marianna Iorio: 0000-0001-8669-5875

Notes

The authors declare no competing financial interest.

■ ACKNOWLEDGMENTS

We would like to thank R. Fattori for adequate and inadequate NMR experiments and for technical advice. We are also grateful to M. Ornaghi for initial work on strain cultivation, to C. Oliva for the EPR spectra, and to E. Wellington for advice. This work was partially supported by the European Community's Seventh Framework Programme (FP7/2007-2013) under Grant Agreement No. 289285 and by grants from Regione Lombardia.

■ REFERENCES

(1) WHO, W. H. O. *Antimicrobial resistance: global report on surveillance 2014*; World Health Organization, 2014.

(2) Cragg, G. M.; Newman, D. J. *Biochim. Biophys. Acta, Gen. Subj.* **2013**, *1830*, 3670−3695.

(3) Monciardini, P.; Iorio, M.; Maffioli, S.; Sosio, M.; Donadio, S. *Microb. Biotechnol.* **2014**, *7*, 209−220.

(4) Pozzi, R.; Simone, M.; Mazzetti, C.; Maffioli, S.; Monciardini, P.; Cavaletti, L.; Bamonte, R.; Sosio, M.; Donadio, S. *J. Antibiot.* **2011**, *64*, 133−139.

(5) Mazzetti, C.; Ornaghi, M.; Gaspari, E.; Parapini, S.; Maffioli, S.; Sosio, M.; Donadio, S. *J. Nat. Prod.* **2012**, *75*, 1044−1050.

(6) Cruz, J. C.; Iorio, M.; Monciardini, P.; Simone, M.; Brunati, C.; Gaspari, E.; Maffioli, S. I.; Wellington, E.; Sosio, M.; Donadio, S. *J. Nat. Prod.* **2015**, *78*, 2642−2647.

(7) Cruz, J. C. S.; Maffioli, S. I.; Bernasconi, A.; Brunati, C.; Gaspari, E.; Sosio, M.; Wellington, E.; Donadio, S. *J. Antibiot.* **2016**, 1−6.

(8) Tamura, T.; Ishida, Y.; Nozawa, Y.; Otoguro, M.; Suzuki, K. *Int. J. Syst. Evol. Microbiol.* **2009**, *59*, 1867−1874.

(9) Shin-ya, K.; Furihata, K.; Teshima, Y.; Hayakawa, Y.; Seto, H. *Tetrahedron Lett.* **1992**, *33*, 7025−7028.

(10) Hilton, B. D.; Misra, R.; Zweier, J. L. *Biochemistry* **1986**, *25*, 5533−5539.

(11) Gould, S. J.; Melville, C. R. *Tetrahedron Lett.* **1997**, *38*, 1473−1476.

(12) Ameer, F.; Giles, R. G. F.; Green, I. R.; Pearce, R. *Synth. Commun.* **2004**, *34*, 1247−1258.

(13) Wurm, G.; Gurka, H. J.; Geres, U. *Arch. Pharm. (Weinheim, Ger.)* **1986**, *319*, 1106−1113.

(14) Wu, K.-L.; Mercado, E. V.; Pettus, T. R. R. *J. Am. Chem. Soc.* **2011**, *133*, 6114−6117.

(15) Ogawa, H.; Natori, S. *Chem. Pharm. Bull.* **1968**, *16*, 1709−1720.

(16) Cameron, D. W.; Cromartie, R. I. T.; Kingston, D. G. I.; Todd, L. *J. Chem. Soc.* **1964**, *0*, 51−61.

(17) Kulanthaivel, P.; Perun, T. J.; Belvo, M. D.; Strobel, R. J.; Paul, D. C.; Williams, D. C. *J. Antibiot.* **1999**, *52*, 256−262.

(18) Liu, B.; Tan, Y.; Gan, M. L.; Zhou, H. X.; Wang, Y. G.; Ping, Y. H.; Li, B.; Yang, Z. Y.; Xiao, C. L. *Acta Pharm. Sin. B* **2014**, *49*, 230−236.

(19) Cruz, J. S. C. *Unlocking the potential of novel taxa: a study on Actinoallomurus*. Ph.D. Thesis; University of Warwick, Warwick, UK, 2016.

(20) Rafanan, E.; Le, L.; Zhao, L.; Decker, H.; Shen, B. *J. Nat. Prod.* **2001**, *64*, 444−449.

(21) Ames, B. D.; Korman, T. P.; Zhang, W.; Smith, P.; Vu, T.; Tang, Y.; Tsai, S.-C. *Proc. Natl. Acad. Sci. U. S. A.* **2008**, *105*, 5349−5354.

(22) Daum, M.; Peintner, I.; Linnenbrink, A.; Frerich, A.; Weber, M.; Paululat, T.; Bechthold, A. *ChemBioChem* **2009**, *10*, 1073−1083.

(23) Tocchetti, A.; Maffioli, S.; Iorio, M.; Alt, S.; Mazzei, E.; Brunati, C.; Sosio, M.; Donadio, S. *Chem. Biol.* **2013**, *20*, 1067−1077.

(24) Monciardini, P.; Sosio, M.; Cavaletti, L.; Chiocchini, C.; Donadio, S. *FEMS Microbiol. Ecol.* **2002**, *42*, 419−429.

(25) Weber, T.; Blin, K.; Duddela, S.; Krug, D.; Kim, H. U.; Bruccoleri, R.; Lee, S. Y.; Fischbach, M. A.; Müller, R.; Wohlleben, W.; Breitling, R.; Takano, E.; Medema, M. H. *Nucleic Acids Res.* **2015**, *43*, 1−7.

(26) Medema, M. H.; Kottmann, R.; Yilmaz, P.; Cummings, M.; Biggins, J. B.; Blin, K.; de Bruijn, I.; Chooi, Y. H.; Claesen, J.; Coates, R. C.; Cruz-Morales, P.; Duddela, S.; Dusterhus, S.; Edwards, D. J.;

Fewer, D. P.; Garg, N.; Geiger, C.; Gomez-Escribano, J. P.; Greule, A.; Hadjithomas, M.; Haines, A. S.; Helfrich, E. J. N.; Hillwig, M. L.; Ishida, K.; Jones, A. C.; Jones, C. S.; Jungmann, K.; Kegler, C.; Kim, H. U.; Kotter, P.; Krug, D.; Masschelein, J.; Melnik, A. V.; Mantovani, S. M.; Monroe, E. A.; Moore, M.; Moss, N.; Nutzmann, H.-W.; Pan, G.; Pati, A.; Petras, D.; Reen, F. J.; Rosconi, F.; Rui, Z.; Tian, Z.; Tobias, N. J.; Tsunematsu, Y.; Wiemann, P.; Wyckoff, E.; Yan, X.; Yim, G.; Yu, F.; Xie, Y.; Aigle, B.; Apel, A. K.; Balibar, C. J.; Balskus, E. P.; Barona-Gomez, F.; Bechthold, A.; Bode, H. B.; Borriss, R.; Brady, S. F.; Brakhage, A. A.; Caffrey, P.; Cheng, Y.-Q.; Clardy, J.; Cox, R. J.; De Mot, R.; Donadio, S.; Donia, M. S.; van der Donk, W. A.; Dorrestein, P. C.; Doyle, S.; Driessen, A. J. M.; Ehling-Schulz, M.; Entian, K.-D.; Fischbach, M. A.; Gerwick, L.; Gerwick, W. H.; Gross, H.; Gust, B.; Hertweck, C.; Hofte, M.; Jensen, S. E.; Ju, J.; Katz, L.; Kaysser, L.; Klassen, J. L.; Keller, N. P.; Kormanec, J.; Kuipers, O. P.; Kuzuyama, T.; Kyrpides, N. C.; Kwon, H.-J.; Lautru, S.; Lavigne, R.; Lee, C. Y.; Linquan, B.; Liu, X.; Liu, W.; Luzhetskyy, A.; Mahmud, T.; Mast, Y.; Mendez, C.; Metsa-Ketela, M.; Micklefield, J.; Mitchell, D. A.; Moore, B. S.; Moreira, L. M.; Muller, R.; Neilan, B. A.; Nett, M.; Nielsen, J.; O'Gara, F.; Oikawa, H.; Osbourn, A.; Osburne, M. S.; Ostash, B.; Payne, S. M.; Pernodet, J.-L.; Petricek, M.; Piel, J.; Ploux, O.; Raaijmakers, J. M.; Salas, J. A.; Schmitt, E. K.; Scott, B.; Seipke, R. F.; Shen, B.; Sherman, D. H.; Sivonen, K.; Smanski, M. J.; Sosio, M.; Stegmann, E.; Sussmuth, R. D.; Tahlan, K.; Thomas, C. M.; Tang, Y.; Truman, A. W.; Viaud, M.; Walton, J. D.; Walsh, C. T.; Weber, T.; van Wezel, G. P.; Wilkinson, B.; Willey, J. M.; Wohlleben, W.; Wright, G. D.; Ziemert, N.; Zhang, C.; Zotchev, S. B.; Breitling, R.; Takano, E.; Glockner, F. O. *Nat. Chem. Biol.* **2015**, *11*, 625−631.

(27) Clinical and Laboratory Standards Institute. M100-S26: *Performance standards for antimicrobial susceptiblity testing*, 26th ed.; Wayne, PA, 2016; p 256.

DOI: 10.1021/acs.jnatprod.6b00654
J. Nat. Prod. 2017, 80, 819−827